

---

## Kinetics of monoclonal anti-epidermal growth factor receptor antibody (IOR EGF/R3)-induced apoptosis in human carcinoma bearing nude mice

JORGE DUCONGÉ, Ph D\*; NELSON MERINO, Ph D\*; DALIA ALVAREZ, MD\*; IRENE BEAUSOLEIL, MS†; EDUARDO FERNÁNDEZ-SÁNCHEZ, Ph D\*; LEYANIS RODRÍGUEZ, MS\*; ALASTAIR D. BURT, Ph D‡

---

**Apoptosis seems to play an important role in cancer immunotherapy outcome. We have studied the kinetic pattern of apoptosis induction in H125 human lung carcinoma xenografts after treatment with the monoclonal antibody (MAB) anti-epidermal growth factor receptor (EGFr) IOR EGF/r3. Tumor-bearing nude mice were injected intravenously with a single 8 mg/kg dose of IOR EGF/r3 and tumor specimens were taken up to 30 days post treatment. Apoptosis was measured by morphometric analysis of the histological sections at each tumor specimen over time points. The results showed a significant apoptotic response in tumors within six days after injection of this MAB**

**reaching a peak at 20 days post treatment. The kinetics were very broad, with apoptotic cells present over the entire time-frame. However, the time course of the apoptotic index showed a significant difference to the mitotic index. Finally, the MAB-induced apoptosis was related to tumor growth delay indicating a probable arrest of cell cycle and a corresponding inhibition of tumor progression, which was corroborated by the Ki67 and proliferating cell nuclear antigen (PCNA) biomarkers.**

*Key words: Immunotherapy, Tumor xenograft, Apoptosis, Tumor growth delay.*

---

Programmed cell-death is a physiological mode of cell deletion that has received heightened attention in recent years as its fundamental role in a number of biological processes has been recognized. Cell death by apoptosis has been implicated in a number of human diseases, including malignancy (1). Loss of apoptotic propensity may be an early step in oncogenesis, allowing the survival of cells following otherwise lethal DNA damage and thereby propagating the additional genetic alterations that lead to malignancy (2). Moreover, apoptosis may be a major mode of cell death in response to modalities used in cancer treatment (1), and the possibility that apoptosis may be enhanced in tumors for therapeutic benefit has stimulated a great deal of research to modulate this process (3).

It has been known for many years that cells with the characteristic morphological features of apoptosis appear

in tumor tissues after exposure to both ionizing radiation and chemotherapeutic agents (4). Much of the data have derived from studies performed involving cells cultured in vitro. Studies of treatment-induced apoptosis in vivo have been sparse; even so, morphometric analysis of tumors treated in situ with radiation (5) or growth hormone deprivation (6) have illustrated that these agents produce an apoptotic response with time course and dose-response relationships characteristic of the particular agent and tumor examined.

It was difficult to evaluate from these early studies how significant was the small ratio of cells dying by this means with regard to tumor response. However, it is now known that apoptosis may be an important pathway for cell loss even in untreated tumors and that an apoptotic index (AI) of just a few percentage represents a large rate of cell turnover (7). Thus, a complete assessment of the role of apoptosis in tumor response to therapy must await a more complete description of the kinetics of apoptotic induction in treated tumors.

One possible therapeutic approach to the treatment of malignant tumors is the use of antibodies against growth factor-activated receptors. In the case of the MAB IOR EGF/r3, we have postulated a potential apoptosis inducer role according to some results observed in both in vitro and in vivo experimental systems (8), and in correspondence with its blocking activity upon binding

---

\* Department of Pharmacology & Toxicology, Center for Biological Evaluation and Research Institute of Pharmacy & Foods, University of Havana, Havana 36, CP 13600, Cuba, †Center of Molecular Immunology, Havana, PO Box 16040, CP 11600, Cuba. ‡Department of Pathology, Royal Victoria Infirmary, University of Newcastle upon Tyne, NE1 4LP, United Kingdom.

Address correspondence to: Jorge Ducongé, Ph D, Department of Pharmaceutical Sciences, Suite 413C, School of Pharmacy, Medical Sciences Campus, University of Puerto Rico, PO Box 365067, San Juan PR 00936-5067, Phone (787) 758 2525 (ext. 5433), Fax (787) 7672796, e-mails: jduconge@rcm.upr.edu

of the epidermal growth factor (EGF) and EGF-like peptides to the EGFr. In fact, the murine monoclonal antibody anti-EGFr IOR EGF/r3 (IgG<sub>2a</sub> isotype) recognizes two conformational sequence-sites of the EGFr extracellular domain, with binding affinity comparable to the natural ligand ( $K_d=10^{-9}$  M), and competes with ligand binding and receptor tyrosine kinase activation in intact tumor cells(9).

The aim of this study was to assess the kinetic pattern of the in vivo apoptotic response induced by the MAB IOR EGF/r3 in non-small cell human lung carcinoma and correlate it with tumor growth.

## Materials and Methods

**Drug:** The murine MAb anti-EGFr IOR EGF/r3, manufactured by the Center of Molecular Immunology, (Havana, Cuba), has been produced conforming to the standard of quality for injectable formulations. Each vial contains 50 ( $\pm 0.2$ ) mg of sterile MAb IOR EGF/r3 powder in 10 ml of neutral phosphate-buffered saline (PBS) solution.

**Animal Husbandry:** Male NmRI/ nu-nu strain nude mice (8-10 weeks old, mean weight  $25 \pm 3$  g) were housed as a group and were bred and maintained under controlled conditions during the experiment. Access to food and water was provided ad libitum to all animals. All studies were approved by the Institutional Animal Care and Use Committee and were performed in accordance with the guidelines of the good laboratory procedures for animal use and welfare. According to the experimental design, all these immunosuppressed animals were randomly separated into two groups: The MAb-treated group and the non-drug PBS-treated control group. Three animals at each time point were considered in both groups.

**Tumor Cell Line:** The HER2/neu-overexpressing cell line, H125, from a non-small cell human lung carcinoma was used. This tumor line was expanded in RPMI 1690 media (SEROMED, Berlin, FRG) supplied with 10% FBS (GIBCO, BRL, UK), 100mg/ml penicillin and 100mg/ml streptomycin. The media was maintained at 37° C and 5% CO<sub>2</sub> conditions.

**Tumor-bearing Nude Mice:** Solitary tumors were produced in the right abdominal flank by subcutaneous inoculation of  $2 \times 10^6$  viable tumor cells in 0.1 ml of medium. These transplantable tumors are non-immunogenic to these hosts and therefore grow without rejection. They were submitted to the study when the xenografts had grown up to approximately 0.5 cm<sup>3</sup> of average diameter ( $\varnothing_{av}$ ), according to the following expression:  $\varnothing_{av} = (\pi/6) \cdot ab^2$ , where a (length) is the largest and b (width) is the shortest tumor diameter. Each diameter was measured using a vernier caliper.

**Kinetics Assay:** The MAb-treated group was dosed by a single 8 mg/kg intravenous bolus input (via ocular plexus) of the MAb IOR EGF/r3, whereas the control group received intravenously the same volume (0.1 ml) of PBS.

The mice were killed by cervical dislocation on day 0 (pre-dose) and at 2; 6; 15; 20; and 30 days after treatment. Tumor specimens were immediately excised and placed in 4% buffered formalin for apoptosis and mitosis measurements using morphometric methods. The tissue was processed for embedding in paraffin blocks, from which 2 to 4 $\mu$ m sections were cut and stained with hematoxylin (H) and eosin (E). The morphological features were then used for histological identification of both mitosis and apoptosis, the latter being distinguished from necrosis as described in earlier publications (5, 10).

Apoptosis was scored in coded slides by microscopic examination of H and E-stained sections at 400X magnification. To determine both the apoptotic index (AI) and the mitotic index (MI), 5 fields of non-necrotic areas were selected in each specimen, and in each field the numbers of apoptotic and mitotic cells were recorded to reach 1000 cells and expressed as a percentage. The calculated values of both AI and MI were based on scoring 15 000 cells (5 000 cells per animal), obtained from three mice per time point within each group.

**Tumor Size:** For tumor growth delay analysis, the tumor size of both PBS and MAb-treated group was followed-up measuring two mutually orthogonal tumor diameters, by triplicate in each animal, and calculating the corresponding average diameter as mentioned above. Measurements were performed on day 0 (pre-dose) and at 1; 2; 6; 15; 18; 20; 22; 28 and 30 days after treatment.

**Proliferation Biomarkers:** To this end, the corresponding commercial kits (Novo Castra Laboratories Ltd., Newcastle upon Tyne, UK) for immunohistochemistry were used. Each kit was developed for assessing cell proliferation by the detection of either Ki67 antigen or PCNA in paraffin-embedded sections of each tumor specimen, utilizing avidin and biotinylated horseradish peroxidase complex technology. Typical working dilution was 1:100–1:200. Each staining run was based on either a specific monoclonal anti-Ki67 antibody (NCL-Ki67-MM1) or a specific monoclonal anti-PCNA antibody (NCL-PCNA) for immunohistochemical staining of tumor specimens at each time points. Briefly, 5 fields of non-necrotic areas were selected in each specimen, and up to 1000 cells were recorded in each field. The calculated values for both biomarkers, expressed as a percentage, were based on scoring 15 000 cells (5 000 cells per animal).

**Statistical Analysis:** All data points, from 0 to 30 days after treatment, were expressed as mean and standard deviation (N=15). For both groups under study, normality

(Shapiro- Wilks test) and homogeneity of variance (Levene test) were tested before statistical comparison between groups. Finally, a parametric two-tailed t-test for independent samples was performed with a 5% probability level.

A correlation and multiple regression analysis using ANOVA of regression were performed in order to compare the slope (i.e., tumor growth rate) of the curve from the MAb group to that from the PBS one. In doing so, a two-stage analysis of their slope parameters was accomplished taking into account two time sections of both profiles (i.e., first, from 0 to 2 days and, then, from 6 to 30 days). For all these purposes, the statistical package STATISTIC for Windows (Statsoft. Inc., ver 5.1, 1996) was used.

The tumor growth delay (TGD) ratio, expressed as percentage, was estimated from slope values as follows:  $TGI \text{ ratio} = (S_{Cav} - S_{Dav}) / S_{Cav} \times 100\%$

Where,  $S_{Dav}$  and  $S_{Cav}$  represent the slopes of the best-fitted polynomial functions corresponding to mean data points, within the second time-frame, from the MAb-treated and the PBS control group, respectively. We followed an earlier method of analysis of growth curves, where a full explanation can be found (11). Briefly, the method utilizes the technique of analysis of covariance, but adding the concept of confidence intervals for improvement of polynomial curve fitting to growth data, which yields results identical to those that were obtained by weighting inversely by the sample covariance matrix, but has the additional feature of allowing flexibility in weighting by choosing subsets of covariates. This approach leads to methods of estimating parameters and performing tests that can be easily implemented by standard multivariate linear model programs (11).

## Results

The in vivo kinetics of both apoptosis and mitosis in H125 xenografts, treated with a single intravenous dose of 8 mg/kg, is depicted in Figure 1. No significant effect on extent of cell division, as reflected by the MI after IOR EGF/r3 treatment, is noted during first 20 days, whilst the number of apoptotic bodies per fields on the analyzed specimens demonstrated a significant programmed cell death (PCD) induction.

Enhanced apoptosis became apparent in the treated group within 2 days post MAb injections, reaching a maximum near to this time and then returning to control values at 30 days. It was important to examine whether cell proliferation was affected in a similar manner by the treatment. The percentage of mitosis was scored from the same sections that were analyzed for apoptosis and reported as the mitotic index. Tables 1 and 2 show the

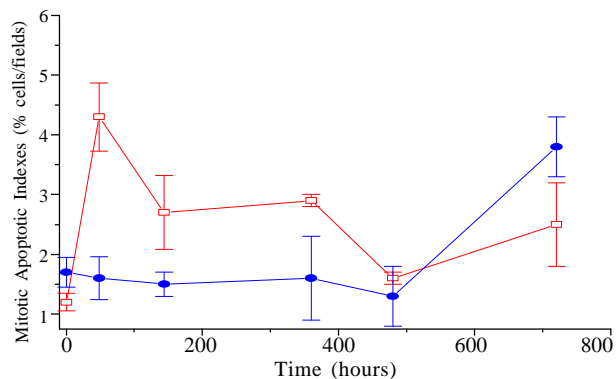


**Figure 1.** Kinetic pattern for both mitotic (solid circle) and apoptotic (open square) responses, expressed as percentage values over 15 000 cells and calculated after a single MAb IOR EGF/r3 dose of 8 mg/kg in tumor bearing nude mice.

values for either AI or MI of both MAb-treated and PBS-treated groups.

As can be seen, in the PBS-treated group (control) there was a small but sustained MI rise over levels at the beginning of experience; whereas, in the MAb-treated

**Table 1.** The statistical analysis was accomplished through comparison of the apoptotic index (AI) between both groups under study. A paired t-student test, with 5% probability, was used. AI values were calculated with regard to 1000 cells.

Time (h)	AI mean values ( $\pm$ S. D.)		p level
	PBS	IOR EGF/r3	
0	1.4 ( $\pm$ 0.2)	1.2 ( $\pm$ 0.2)	NS
48	1.9 ( $\pm$ 0.3)	4.3 ( $\pm$ 0.2)	0.0002
144	1.5 ( $\pm$ 0.4)	2.7 ( $\pm$ 0.7)	0.05
360	1.5 ( $\pm$ 0.2)	2.9 ( $\pm$ 0.1)	0.0004
480	1.6 ( $\pm$ 0.6)	1.6 ( $\pm$ 0.6)	NS
720	2.1 ( $\pm$ 1.1)	2.5 ( $\pm$ 0.7)	NS

NS means no-significant differences between groups.

**Table 2.** Statistical comparison between treated and untreated control group, for Mitotic Index (MI). A paired t-student test, with 5% probability, was used. MI values were calculated with regard to 1000 cells.

Time (h)	MI mean values ( $\pm$ S. D.)		p level
	PBS	IOR EGF/r3	
0	1.8 ( $\pm$ 0.2)	1.7 ( $\pm$ 0.3)	NS
48	1.9 ( $\pm$ 0.3)	1.6 ( $\pm$ 0.4)	NS
144	2.0 ( $\pm$ 0.5)	1.5 ( $\pm$ 0.2)	NS
360	2.5 ( $\pm$ 0.4)	1.6 ( $\pm$ 0.7)	NS
480	2.2 ( $\pm$ 0.6)	1.3 ( $\pm$ 0.5)	NS
720	2.3 ( $\pm$ 0.4)	3.8 ( $\pm$ 0.5)	0.015

NS means no-significant differences between groups.

group an index that slightly dropped below baseline levels and rebounded at 30 days for was accounted . Consequently, the MI attained at this time point was significantly higher in the MAb-treated group than in the control.

Apoptosis produced by IOR EGF/r3 can be compared to its anti-tumor efficacy by reference to the tumor growth curves depicted in Figure 2 and supported by the statistical analysis in Tables 3 and 4. The analysis of the full time course of both curves by comparison between their regression slopes, using ANOVA of regression, showed

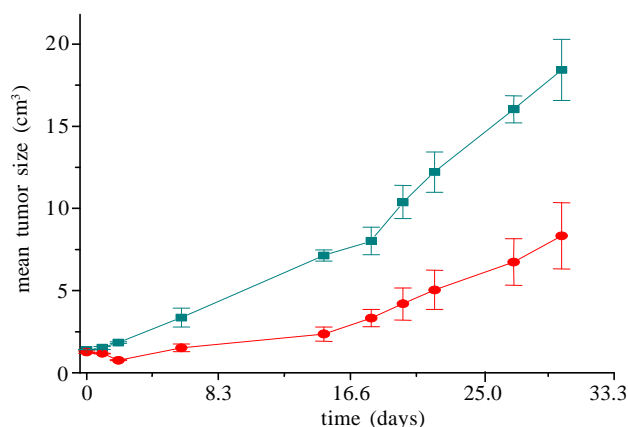


**Figure 2.** Tumor growth curves corresponding to both MAB IOR EGF/r3-treated group (solid circle) with a single intravenous dose (8 mg/kg), and PBS-treated control group (solid square), in tumor bearing nude mice. Kinetics pattern shows a tumor growth delay after IOR EGF/r3 treatment.

that these slopes belong to different family of growth curves ( $p = 0.003$ ). A satisfactory delay of tumor growth rate was shown with a 13% TGD ratio, which denoted a potential of this monoclonal for tumor growth inhibition (see Figure 2), even though significant remission of the tumor mass was not evident over time other than the first 48 hours, as can be derived from negative slope of best fitted polynomial function within 0-48 hours (see Table 4).

Figure 3 depicts photomicrographs of immunohistochemical staining for both Ki67 antigen and PCNA molecule in malignant cells at 48 hours after dosing when higher AI/MI ratio was observed. As can be seen, these two proliferation markers (i.e, Ki67 and PCNA) were better detected in the PBS control rather than in the IOR EGF/r3-treated slices, suggesting a higher AI/MI ratio in the latter and supporting our thesis of IOR EGF/r3-driven induction of any PCD in treated tumors after stopping cell-cycle progression. Table 5 shows the estimated average Ki67 and PCNA values as percentage at each time point according to immunostaining of specimens. Notice the irregular behavior over time from the observed PCNA

**Table 3.** Comparison of tumor growth curves from both groups. Statistical analysis was achieved by correlation and multiple regression analysis of both profiles using a polynomial function as a model.

<b>PBS-treated control group (<math>r^2 = 0.834</math>)</b>				
<b>Slope = <math>9.394 \cdot 10^3 (\pm 1.15 \cdot 10^3)</math></b>				
Variance Source	DF	QSS	F	p
Between groups	9	190.53	31.51	0.001
Regression	1	170.1	66.275	0.001
Deviation of regression	8	20.52	3.819	0.010
Within groups	20	13.43	----	----
<b>Total</b>	<b>29</b>	<b>208.97</b>	----	----

<b>MAB IOR EGF/r3-treated group (<math>r^2 = 0.949</math>)</b>				
<b>Slope = <math>1.345 \cdot 10^2 (\pm 6.56 \cdot 10^4)</math></b>				
Variance Source	DF	QSS	F	p
Between group	9	355.33	65.77	0.001
Regression	1	348.68	419.65	0.001
Deviation of regression	8	6.647	1.384	NS
Within groups	20	12.006	----	----
<b>Total</b>	<b>29</b>	<b>367.34</b>	----	----

DF means degree of freedom; QSS means sum of quadratic standard error; F is Fischer's number; p is probability level; NS means non significant difference.

**Table 4.** Analysis of slopes from both tumor growth curves, by ANOVA of regression, using two sections of both curves, from 0 to 48 hours and from 144 to 720 hours.

Parameters	PBS	MAB IOR EGF/r3	p
<b>[0 to 48 hours]</b>			
Slope	$4.305 \cdot 10^{-3}$	$-1.04 \cdot 10^{-2}$	0.0001
Intercept	1.284	1.308	
<b>[144 to 720 hours]</b>			
Slope	$1.426 \cdot 10^{-2}$	$1.248 \cdot 10^{-2}$	NS
Intercept	0.5047	-1.314	

\*Statistically significant difference between groups was observed during first 48 hours.

marker, which becomes increasingly difficult to make any prediction on tumor response. In fact, these PCNA values lagged behind current phase of cell cycle, overestimating actual cell proliferation in comparison with Ki67 antigen detection. Conversely, the Ki67 marker permitted us to postulate a pattern in relation to the previously observed MI and also tumor growth time courses.

A moderate degree of inverse correlation between Ki67 antigen and AI to MI ratio was observed in the MAB-treated group, which yielded new evidence concerning the idea of postulating IOR EGF/r3 as an inducer of cell-

**Table 5.** Statistical comparison between treated and untreated control group, for both PCNA and Ki67 antigen. A paired t-student test, with 5% probability, was used. PCNA and Ki67 values were calculated with regard to 1000 cells.

Time (h)	PCNA mean values ( $\pm$ SD)		p level	Ki67 mean values ( $\pm$ SD)		p level
	PBS	IOR EGF/r3		PBS	IOR EGF/r3	
0	5.7 ( $\pm$ 1.2)	6.2 ( $\pm$ 0.8)	NS	2.9 ( $\pm$ 0.7)	3.4 ( $\pm$ 0.5)	NS
48	6.2 ( $\pm$ 1.1)	11.1 ( $\pm$ 1.6)	0.012	2.2 ( $\pm$ 0.8)	1.3 ( $\pm$ 0.6)	NS
144	9.4 ( $\pm$ 0.8)	3.7 ( $\pm$ 0.4)	0.002	3.8 ( $\pm$ 1.2)	1.2 ( $\pm$ 0.4)	0.024
360	7.5 ( $\pm$ 1.4)	4.3 ( $\pm$ 0.7)	0.038	4.2 ( $\pm$ 0.7)	2.1 ( $\pm$ 0.7)	0.021
480	9.5 ( $\pm$ 0.6)	3.1 ( $\pm$ 0.3)	0.001	4.7 ( $\pm$ 0.5)	2.1 ( $\pm$ 0.6)	0.004
720	10.2 ( $\pm$ 1.4)	5.6 ( $\pm$ 1.5)	0.018	6.1 ( $\pm$ 1.2)	1.8 ( $\pm$ 1.0)	0.009

NS means no-significant differences between groups.

cycle arrest and pro-apoptotic response, even though MI values were determined following morphometric analysis whereas immunostaining for Ki67 antigen often picks out a maximum label at G<sub>2</sub>/M boundary of the cell cycle. Notably, Ki67 values in the MAb-treated group declined

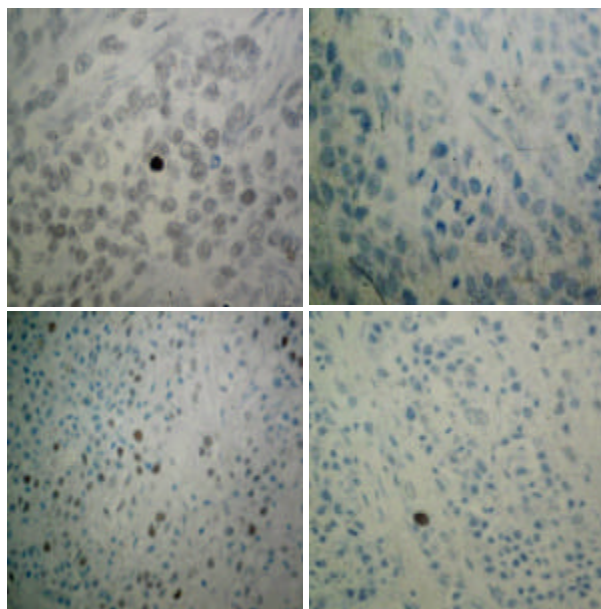


**Figure 3.** Immunohistochemical staining for both Ki67 antigen using NCL-Ki67-MM1 (upper panels) and PCNA using NCL-PCNA (lower panels), in tumor specimen from either PBS-treated control (left hand) or IOR EGF/r3-treated (right hand) xenograft, 48 hours after dosing. Paraffin sections. Note intense nuclear staining of proliferating H125 cells, particularly in controls.

below baseline up to about 144 hours after treatment and then recovered from day 15 onward. As expected, such proliferation markers confirmed the assumptions derived from former AI/MI assessments.

## Discussion

Little is known of the role of PCD in the response of tumors to different therapeutic modalities in spite of the fact that almost 30 years ago cells with the features of apoptosis were demonstrated in the tumors of treated animals (12). Much of what has been done in recent years has primarily involved cells treated in vitro. Although, much has been learned about basic mechanisms from such studies, a critical question that remains

unanswered is whether these mechanisms extrapolate to tumors treated in vivo. This study was conducted to assess the magnitude and time course of the apoptosis induction in carcinomas treated with a promising agent (viz, monoclonal antibody IOR EGF/r3), in order to determine whether this mode of cell death can be involved in its therapeutic action.

Earlier summaries of in vivo studies on HiFi colon adenocarcinomas, at the Sloan Kettering Cancer Center of New York, report that these tumor cells display the features of apoptosis following exposure to the anti-EGFr human-to-murine chimeric MAb C225 (13). Furthermore, in vitro studies on cultured H125 cells showed the presence of apoptotic bodies following IOR EGF/r3 treatment and, more recently, in vivo studies using both murine IOR EGF/r3 and its humanized version showed similar pro-apoptotic pattern on A431 cells (8). Nonetheless, it has also been shown that the appearance of apoptosis in treated cells is a very dynamic and complex process, making it difficult to readily assess the total proportion of apoptotic cells.

The kinetics of apoptosis induction by IOR EGF/r3 in the H125 cells, confirms that several factors may contribute to the proportion of apoptotic cells visualized at any time point. This kinetic pattern is in contrast to that seen after ionizing radiation and other therapy options (10, 14). One explanation may be the pharmacokinetics of the drug uptake by the tumor cells, which probably occurs asynchronously and over a longer time compared to radiation, where the entire dose is delivered within a few minutes.

Alternatively, the kinetics of apoptosis following MAb treatment may be due to cell cycle specificity for induction of this mode of cell death as suggested by Barry et al. (15). It is possible that there are other modes of cell death and that a high proportion of cells in these tumors died by what is referred to as reproductive cell death, where cells simply stop dividing after completing one or more abnormal post treatment divisions. It is not clear that this mode of

cell death occurs in these tumors since it cannot be visualized. However, it is consistent with the fact that the MI fell below the levels before IOR EGF/r3 injection and displayed a plateau during the next 20 days, and then suddenly showed a rapid recovery.

A possible explanation for this terminal proliferation behavior is related to the heterogeneous angio-architecture of these tumors and therefore the heterogeneous distribution of macromolecules into these tumors, as previously was suggested (16-18), along with the better condition found by resistant clones for their malignancy due to death of the treated sensitive ones. It reinforces the requirements of multiple dosage regimens in order to obtain sustained steady-state drug levels over longer time periods, that permit us a complete saturation of the over-expressed EGFr on target tumor cells. In this context, we firmly believe that using chemotherapy along with IOR EGF/r3 immunotherapy should yield a better global clinical outcome.

The AI observed at any specific time most likely underestimates the total proportion of cells that undergo apoptosis throughout the time course of the experiment. This might be due to the fact that two competing processes are going on: as apoptotic cells are continuously formed they are quickly phagocytosed, perhaps accounting for the ultimate decline in AI observed after the peak near to 20 days. Thus, the true proportion of cells deleted through apoptosis may be much higher, considering that the life time for visualization of an apoptotic cell may be as short as 3 hours (19). Moreover, some tumor cells may be resistant to apoptosis; it is now well established from a number of studies that the propensity for apoptosis in response to a variety of agents used in cancer therapy, including MABs against EGFr, is highly dependent on the oncogenic status of the cell.

The effects of IOR EGF/r3 on tumor growth were measured to test the role of apoptosis on tumor response. All treated tumors displayed a fairly evident growth delay after a single dose of 8 mg/kg. However, the exact relationship between apoptosis induction and this tumor response measured in terms of growth delay is not clear; nevertheless, this dose counteracted the tumor mass progression compared to the control group, but they continued to grow after a slight delay even though substantial apoptosis was induced with this dose. There are two possible explanations for this apparent discrepancy. First, as discussed above, the evaluation of apoptosis from the histological sections may underestimate the total proportion of cells that underwent apoptosis during the time course studied. Second, since the re-growth kinetics also depend strongly on the rates of proliferation of surviving clones, apoptosis in the tumors

that received a single dose could be offset by new cell division of these surviving clones after clearance of the monoclonal antibody. The MI scored on the same sections as used for the analysis of apoptosis confirmed that cell proliferation was suppressed to a not very high extent and rebounded near 30 days. Thus, resumption of spontaneous apoptosis in these tumors apparently relied on resumption of cell proliferation.

The assessment of cell proliferation by detection of Ki67 antigen has been shown to be of some prognostic value. NCL-Ki67-MM1 label Ki67 antigen in the granular components of the nucleolus during late G1, S, G2 and M phases of cell cycle, and several reports have suggested that there is a strong correlation between Ki67 index and grade histopathology of tumors. Interestingly, the prognosis of this cell-cycle associated marker has been found comparable to [ $H^3$ ] thymidine assay as a sound cell proliferation criterion.

On the other hand, PCNA is a 36 kDa protein which is highly conserved between species and functions as a cofactor for DNA polymerase delta in both S phase and also in DNA synthesis associated with DNA damage repair mechanism. Yet, PCNA may also be detected in non-cycling cells at G0 phase inasmuch as this molecule has a half-life in excess of 20 hours. Therefore, these values on Table 5 should be seen with caution for further interpretation.

It now appears that PCNA is also a communication point between a variety of important cellular processes including cell cycle control, DNA replication, and at least one apoptotic pathway. The dynamic movement of PCNA on and off the DNA renders this protein an ideal communicator for a variety of proteins that are essential for DNA metabolic events in eukaryotic cells (20). Even though the primary function of PCNA may be to act as a processivity factor for polymerases, a cell decision as to what type of DNA synthesis has to be carried out for its survival might be addressed by the various interactions of PCNA with other proteins. This eventually leads to decisions such as the direction of PCNA towards faithful replication (preceding cell division), various types of repair processes, or even a stop in DNA synthesis events (cell cycle arrest) that could determine a final cell decision to go into PCD pathway, thus allowing a fine tuning of the interplay of these cardinal processes. We have to learn more about the details of the interactions between PCNA and the various components of cell cycle and how they are regulated.

In summary, we have confirmed the observations of others with regard to the apoptosis inducing properties of the MAB IOR EGF/r3 and extended these observations to the in vivo situation using the tumor bearing nude mice as a relevant animal model at disease-state. The magnitude

of this effect implies that this mode of cell death could play a role in tumor response, especially in tumor delay following treatment with IOR EGF/r3. Thus, understanding the pathways responsible for regulating the propensity for tumor cells to undergo apoptosis as well as its kinetics behaviors could ultimately enable the design of strategies for modulating PCD according to the optimization of IOR EGF/r3's dosage regimens with therapeutic advantage.

## Resumen

La apoptosis tiene un importante papel en la inmunoterapia del cáncer. En este estudio, hemos caracterizado la cinética de inducción de apoptosis en xeno-injertos de carcinoma de pulmón humano, línea tumoral H-125, luego de administrar el anticuerpo monoclonal anti-factor de crecimiento epidérmico IOR EGF/r3. Ratones atómicos que portan un tumor recibieron intravenosamente una dosis única de 8mg/kg de IOR EGF/r3, posteriormente se tomaron muestras del tumor hasta los 30 días siguientes al tratamiento. La apoptosis fue medida mediante análisis morfológico de las secciones histológicas correspondientes a cada muestra de tumor para el intervalo de muestreo establecido. Los resultados muestran una significativa apoptosis en los tumores en los 6 días siguientes a la administración del monoclonal, alcanzando un máximo a los 20 días postratamiento. La respuesta cinética resultó bien extendida, con visualización de células en apoptosis durante todo el período de muestreo. El transcurso temporal del índice de apoptosis muestra una diferencia significativa respecto al índice mitótico. Finalmente, la apoptosis inducida por este monoclonal fue relacionada con el retardo del crecimiento tumoral, indicándose un probable arresto del ciclo celular y una consecuente inhibición de la progresión tumoral, lo cual fue corroborado por los bio-marcadores PCNA y Ki67.

## Acknowledgments

This work was supported by the Center of Molecular Immunology, the Department of Pathology, Royal Victoria Infirmary, University of Newcastle upon Tyne, and in part by grant A023 from Alma Mater project. The skillful technical assistance of Mrs. Amelia Capote, Mr. Armando López, and Mr. Dariel Morales is gratefully acknowledged.

## References

1. Kerr JFR, Winterford CM, Harmon BV. Apoptosis: Its significance in cancer and cancer therapy. *Cancer*, 1994;73: 2013-26.

2. Lane DP. A death in the life of p53. *Nature (Lond.)*, 1993;362: 786-7.
3. Hsu B, Marin MC, Brisbay S, McConnell K, McDonnell TJ. Expression of bcl-2 gene confers multi-drug resistance to chemotherapy-induced cell death. *Cancer Bull.* 1994;46: 125-9.
5. Stephens LC, Ang KK, Schultheiss TE, Milas L, Meyn RE. Apoptosis in irradiated murine tumors. *Rad. Res.* 1991;127: 308-16.
6. Kyprianou N, English HF, Isaacs JT. Programmed cell death during regression of PC-82 human prostate cancer following androgen ablation. *Cancer Research.* 1990;50:3748-53.
7. Arends MJ, McGregor AH, Wyllie AH. Apoptosis is inversely related to necrosis and determines net growth in tumors bearing constitutively expressed myc, ras, and HPV oncogenes. *Am. J. Pathology.* 1994;144:1045-57.
8. Crombet T, Rak J, Perez R, Vilorio-Petit A. Antiproliferative, antiangiogenic and proapoptotic activity of hR3: A humanized anti-EGFr antibody. *Int. J. Cancer.* 2002;101(6):567-575.
9. Fernández A, Pérez R, Macías A, Velanda A, Álvarez I, Ramos M, Velozo A. Generación y caracterización primaria de anticuerpos monoclonales contra el receptor del factor de crecimiento epidérmico. *Interferón y Biotecnología.* 1989; 6(3):289-298.
10. Meyn RE, Stephens LC, Hunter NR, Milas L. Kinetics of cisplatin-induced apoptosis in murine mammary and ovarian adenocarcinomas. *Int. J. Cancer.* 1995;60:725-29.
11. Grizzle JE, Allen DM. Analysis of growth and dose response curves. *Biometrics* 1969;25:357- 81.
12. Searle J, Lawson TA, Abbott PJ. An electron- microscope study of the mode of cell death induced by cancer chemotherapeutic agents in populations of proliferating normal and neoplastic cells. *J. Pathology* 1975;116:129-38.
13. Wu XP, Rubin M, Fan Z, Deblasio T, Soos T, Koff A, Mendelsohn J. Involvement of P27(KIP1) in G(1) arrest mediated by an anti- epidermal growth factor receptor monoclonal antibody. *Oncogene* 1996;12(7):1397-1403.
14. Stephens LC, Hunter NR, Ang KK, Milas L, Meyn RE. Development of apoptosis in irradiated murine tumors as a function of time and dose. *Rad. Res.* 1993;135:75-80.
15. Barry MA, Behnke CA, Eastman A. Activation of programmed cell death by cisplatin, other anticancer drugs, toxins and hyperthermia. *Biochemistry and Pharmacology* 1990;40:2353-62.
16. Ahlstrom H. Anatomy and permeability of tumor vessels. An experimental study in nude rats with the aim of increasing the uptake of MAb anti- CEA in human colonic cancer. PhD Thesis, Department of Diagnostic. Uppsala University, 1988;S-75185, ISBN 91-7900-448-2, Sweden.
17. Jain RK, Baxter LT. Mechanism of heterogeneous distribution of MAb and other macromolecules in tumors: Significance of elevated interstitial pressure. *Cancer Research* 1988;48:7022-32.
18. Jain RK. Physiological barriers to delivery of MAb and other macromolecules in tumors. *Cancer Research* 1990;50:814-19.
19. Bursch W, Paffe S, Putz B, Barthel G, Schulte-Hermann R. Determination of the length of the histological stages of apoptosis in normal liver and in altered hepatic foci of rats. *Carcinogenesis* 1990;11:847-53.
20. Jónsson ZO, Hübscher U. Proliferating cell nuclear antigen: more than a clamp for DNA polymerases. *Bioessays* 1997; 19(11):967-975.

---

## Kinetics of monoclonal anti-epidermal growth factor receptor antibody (IOR EGF/R3)-induced apoptosis in human carcinoma bearing nude mice

JORGE DUCONGÉ, Ph D\*; NELSON MERINO, Ph D\*; DALIA ALVAREZ, MD\*; IRENE BEAUSOLEIL, MS†; EDUARDO FERNÁNDEZ-SÁNCHEZ, Ph D\*; LEYANIS RODRÍGUEZ, MS\*; ALASTAIR D. BURT, Ph D‡

---

**Apoptosis seems to play an important role in cancer immunotherapy outcome. We have studied the kinetic pattern of apoptosis induction in H125 human lung carcinoma xenografts after treatment with the monoclonal antibody (MAB) anti-epidermal growth factor receptor (EGFr) IOR EGF/r3. Tumor-bearing nude mice were injected intravenously with a single 8 mg/kg dose of IOR EGF/r3 and tumor specimens were taken up to 30 days post treatment. Apoptosis was measured by morphometric analysis of the histological sections at each tumor specimen over time points. The results showed a significant apoptotic response in tumors within six days after injection of this MAB**

**reaching a peak at 20 days post treatment. The kinetics were very broad, with apoptotic cells present over the entire time-frame. However, the time course of the apoptotic index showed a significant difference to the mitotic index. Finally, the MAB-induced apoptosis was related to tumor growth delay indicating a probable arrest of cell cycle and a corresponding inhibition of tumor progression, which was corroborated by the Ki67 and proliferating cell nuclear antigen (PCNA) biomarkers.**

*Key words: Immunotherapy, Tumor xenograft, Apoptosis, Tumor growth delay.*

---

Programmed cell-death is a physiological mode of cell deletion that has received heightened attention in recent years as its fundamental role in a number of biological processes has been recognized. Cell death by apoptosis has been implicated in a number of human diseases, including malignancy (1). Loss of apoptotic propensity may be an early step in oncogenesis, allowing the survival of cells following otherwise lethal DNA damage and thereby propagating the additional genetic alterations that lead to malignancy (2). Moreover, apoptosis may be a major mode of cell death in response to modalities used in cancer treatment (1), and the possibility that apoptosis may be enhanced in tumors for therapeutic benefit has stimulated a great deal of research to modulate this process (3).

It has been known for many years that cells with the characteristic morphological features of apoptosis appear

in tumor tissues after exposure to both ionizing radiation and chemotherapeutic agents (4). Much of the data have derived from studies performed involving cells cultured in vitro. Studies of treatment-induced apoptosis in vivo have been sparse; even so, morphometric analysis of tumors treated in situ with radiation (5) or growth hormone deprivation (6) have illustrated that these agents produce an apoptotic response with time course and dose-response relationships characteristic of the particular agent and tumor examined.

It was difficult to evaluate from these early studies how significant was the small ratio of cells dying by this means with regard to tumor response. However, it is now known that apoptosis may be an important pathway for cell loss even in untreated tumors and that an apoptotic index (AI) of just a few percentage represents a large rate of cell turnover (7). Thus, a complete assessment of the role of apoptosis in tumor response to therapy must await a more complete description of the kinetics of apoptotic induction in treated tumors.

One possible therapeutic approach to the treatment of malignant tumors is the use of antibodies against growth factor-activated receptors. In the case of the MAB IOR EGF/r3, we have postulated a potential apoptosis inducer role according to some results observed in both in vitro and in vivo experimental systems (8), and in correspondence with its blocking activity upon binding

---

\* Department of Pharmacology & Toxicology, Center for Biological Evaluation and Research Institute of Pharmacy & Foods, University of Havana, Havana 36, CP 13600, Cuba, †Center of Molecular Immunology, Havana, PO Box 16040, CP 11600, Cuba. ‡Department of Pathology, Royal Victoria Infirmary, University of Newcastle upon Tyne, NE1 4LP, United Kingdom.

Address correspondence to: Jorge Ducongé, Ph D, Department of Pharmaceutical Sciences, Suite 413C, School of Pharmacy, Medical Sciences Campus, University of Puerto Rico, PO Box 365067, San Juan PR 00936-5067, Phone (787) 758 2525 (ext. 5433), Fax (787) 7672796, e-mails: jduconge@rcm.upr.edu

of the epidermal growth factor (EGF) and EGF-like peptides to the EGFr. In fact, the murine monoclonal antibody anti-EGFr IOR EGF/r3 (IgG<sub>2a</sub> isotype) recognizes two conformational sequence-sites of the EGFr extracellular domain, with binding affinity comparable to the natural ligand ( $K_d=10^{-9}$  M), and competes with ligand binding and receptor tyrosine kinase activation in intact tumor cells(9).

The aim of this study was to assess the kinetic pattern of the in vivo apoptotic response induced by the MAB IOR EGF/r3 in non-small cell human lung carcinoma and correlate it with tumor growth.

## Materials and Methods

**Drug:** The murine MAb anti-EGFr IOR EGF/r3, manufactured by the Center of Molecular Immunology, (Havana, Cuba), has been produced conforming to the standard of quality for injectable formulations. Each vial contains 50 ( $\pm 0.2$ ) mg of sterile MAb IOR EGF/r3 powder in 10 ml of neutral phosphate-buffered saline (PBS) solution.

**Animal Husbandry:** Male NmRI/ nu-nu strain nude mice (8-10 weeks old, mean weight  $25 \pm 3$  g) were housed as a group and were bred and maintained under controlled conditions during the experiment. Access to food and water was provided ad libitum to all animals. All studies were approved by the Institutional Animal Care and Use Committee and were performed in accordance with the guidelines of the good laboratory procedures for animal use and welfare. According to the experimental design, all these immunosuppressed animals were randomly separated into two groups: The MAb-treated group and the non-drug PBS-treated control group. Three animals at each time point were considered in both groups.

**Tumor Cell Line:** The HER2/neu-overexpressing cell line, H125, from a non-small cell human lung carcinoma was used. This tumor line was expanded in RPMI 1690 media (SEROMED, Berlin, FRG) supplied with 10% FBS (GIBCO, BRL, UK), 100mg/ml penicillin and 100mg/ml streptomycin. The media was maintained at 37° C and 5% CO<sub>2</sub> conditions.

**Tumor-bearing Nude Mice:** Solitary tumors were produced in the right abdominal flank by subcutaneous inoculation of  $2 \times 10^6$  viable tumor cells in 0.1 ml of medium. These transplantable tumors are non-immunogenic to these hosts and therefore grow without rejection. They were submitted to the study when the xenografts had grown up to approximately 0.5 cm<sup>3</sup> of average diameter ( $\varnothing_{av}$ ), according to the following expression:  $\varnothing_{av} = (\pi/6) \cdot ab^2$ , where a (length) is the largest and b (width) is the shortest tumor diameter. Each diameter was measured using a vernier caliper.

**Kinetics Assay:** The MAb-treated group was dosed by a single 8 mg/kg intravenous bolus input (via ocular plexus) of the MAb IOR EGF/r3, whereas the control group received intravenously the same volume (0.1 ml) of PBS.

The mice were killed by cervical dislocation on day 0 (pre-dose) and at 2; 6; 15; 20; and 30 days after treatment. Tumor specimens were immediately excised and placed in 4% buffered formalin for apoptosis and mitosis measurements using morphometric methods. The tissue was processed for embedding in paraffin blocks, from which 2 to 4 $\mu$ m sections were cut and stained with hematoxylin (H) and eosin (E). The morphological features were then used for histological identification of both mitosis and apoptosis, the latter being distinguished from necrosis as described in earlier publications (5, 10).

Apoptosis was scored in coded slides by microscopic examination of H and E-stained sections at 400X magnification. To determine both the apoptotic index (AI) and the mitotic index (MI), 5 fields of non-necrotic areas were selected in each specimen, and in each field the numbers of apoptotic and mitotic cells were recorded to reach 1000 cells and expressed as a percentage. The calculated values of both AI and MI were based on scoring 15 000 cells (5 000 cells per animal), obtained from three mice per time point within each group.

**Tumor Size:** For tumor growth delay analysis, the tumor size of both PBS and MAB-treated group was followed-up measuring two mutually orthogonal tumor diameters, by triplicate in each animal, and calculating the corresponding average diameter as mentioned above. Measurements were performed on day 0 (pre-dose) and at 1; 2; 6; 15; 18; 20; 22; 28 and 30 days after treatment.

**Proliferation Biomarkers:** To this end, the corresponding commercial kits (Novo Castra Laboratories Ltd., Newcastle upon Tyne, UK) for immunohistochemistry were used. Each kit was developed for assessing cell proliferation by the detection of either Ki67 antigen or PCNA in paraffin-embedded sections of each tumor specimen, utilizing avidin and biotinylated horseradish peroxidase complex technology. Typical working dilution was 1:100–1:200. Each staining run was based on either a specific monoclonal anti-Ki67 antibody (NCL-Ki67-MM1) or a specific monoclonal anti-PCNA antibody (NCL-PCNA) for immunohistochemical staining of tumor specimens at each time points. Briefly, 5 fields of non-necrotic areas were selected in each specimen, and up to 1000 cells were recorded in each field. The calculated values for both biomarkers, expressed as a percentage, were based on scoring 15 000 cells (5 000 cells per animal).

**Statistical Analysis:** All data points, from 0 to 30 days after treatment, were expressed as mean and standard deviation (N=15). For both groups under study, normality

(Shapiro- Wilks test) and homogeneity of variance (Levene test) were tested before statistical comparison between groups. Finally, a parametric two-tailed t-test for independent samples was performed with a 5% probability level.

A correlation and multiple regression analysis using ANOVA of regression were performed in order to compare the slope (i.e., tumor growth rate) of the curve from the MAb group to that from the PBS one. In doing so, a two-stage analysis of their slope parameters was accomplished taking into account two time sections of both profiles (i.e., first, from 0 to 2 days and, then, from 6 to 30 days). For all these purposes, the statistical package STATISTIC for Windows (Statsoft. Inc., ver 5.1, 1996) was used.

The tumor growth delay (TGD) ratio, expressed as percentage, was estimated from slope values as follows:  
 $TGI \text{ ratio} = (S_{Cav} - S_{Dav}) / S_{Cav} \times 100\%$

Where,  $S_{Dav}$  and  $S_{Cav}$  represent the slopes of the best-fitted polynomial functions corresponding to mean data points, within the second time-frame, from the MAb-treated and the PBS control group, respectively. We followed an earlier method of analysis of growth curves, where a full explanation can be found (11). Briefly, the method utilizes the technique of analysis of covariance, but adding the concept of confidence intervals for improvement of polynomial curve fitting to growth data, which yields results identical to those that were obtained by weighting inversely by the sample covariance matrix, but has the additional feature of allowing flexibility in weighting by choosing subsets of covariates. This approach leads to methods of estimating parameters and performing tests that can be easily implemented by standard multivariate linear model programs (11).

## Results

The in vivo kinetics of both apoptosis and mitosis in H125 xenografts, treated with a single intravenous dose of 8 mg/kg, is depicted in Figure 1. No significant effect on extent of cell division, as reflected by the MI after IOR EGF/r3 treatment, is noted during first 20 days, whilst the number of apoptotic bodies per fields on the analyzed specimens demonstrated a significant programmed cell death (PCD) induction.

Enhanced apoptosis became apparent in the treated group within 2 days post MAb injections, reaching a maximum near to this time and then returning to control values at 30 days. It was important to examine whether cell proliferation was affected in a similar manner by the treatment. The percentage of mitosis was scored from the same sections that were analyzed for apoptosis and reported as the mitotic index. Tables 1 and 2 show the

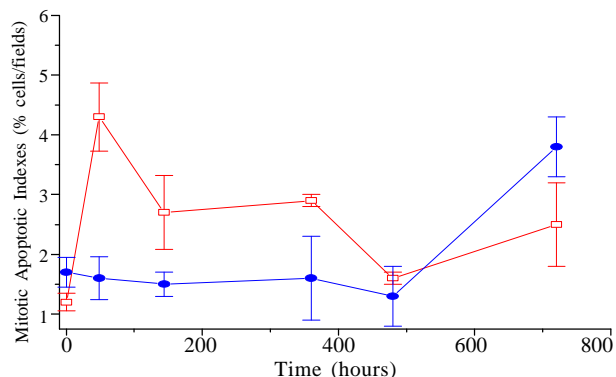


**Figure 1.** Kinetic pattern for both mitotic (solid circle) and apoptotic (open square) responses, expressed as percentage values over 15 000 cells and calculated after a single MAb IOR EGF/r3 dose of 8 mg/kg in tumor bearing nude mice.

values for either AI or MI of both MAb-treated and PBS-treated groups.

As can be seen, in the PBS-treated group (control) there was a small but sustained MI rise over levels at the beginning of experience; whereas, in the MAb-treated

**Table 1.** The statistical analysis was accomplished through comparison of the apoptotic index (AI) between both groups under study. A paired t-student test, with 5% probability, was used. AI values were calculated with regard to 1000 cells.

Time (h)	AI mean values ( $\pm$ S. D.)		p level
	PBS	IOR EGF/r3	
0	1.4 ( $\pm$ 0.2)	1.2 ( $\pm$ 0.2)	NS
48	1.9 ( $\pm$ 0.3)	4.3 ( $\pm$ 0.2)	0.0002
144	1.5 ( $\pm$ 0.4)	2.7 ( $\pm$ 0.7)	0.05
360	1.5 ( $\pm$ 0.2)	2.9 ( $\pm$ 0.1)	0.0004
480	1.6 ( $\pm$ 0.6)	1.6 ( $\pm$ 0.6)	NS
720	2.1 ( $\pm$ 1.1)	2.5 ( $\pm$ 0.7)	NS

NS means no-significant differences between groups.

**Table 2.** Statistical comparison between treated and untreated control group, for Mitotic Index (MI). A paired t-student test, with 5% probability, was used. MI values were calculated with regard to 1000 cells.

Time (h)	MI mean values ( $\pm$ S. D.)		p level
	PBS	IOR EGF/r3	
0	1.8 ( $\pm$ 0.2)	1.7 ( $\pm$ 0.3)	NS
48	1.9 ( $\pm$ 0.3)	1.6 ( $\pm$ 0.4)	NS
144	2.0 ( $\pm$ 0.5)	1.5 ( $\pm$ 0.2)	NS
360	2.5 ( $\pm$ 0.4)	1.6 ( $\pm$ 0.7)	NS
480	2.2 ( $\pm$ 0.6)	1.3 ( $\pm$ 0.5)	NS
720	2.3 ( $\pm$ 0.4)	3.8 ( $\pm$ 0.5)	0.015

NS means no-significant differences between groups.

group an index that slightly dropped below baseline levels and rebounded at 30 days for was accounted . Consequently, the MI attained at this time point was significantly higher in the MAb-treated group than in the control.

Apoptosis produced by IOR EGF/r3 can be compared to its anti-tumor efficacy by reference to the tumor growth curves depicted in Figure 2 and supported by the statistical analysis in Tables 3 and 4. The analysis of the full time course of both curves by comparison between their regression slopes, using ANOVA of regression, showed

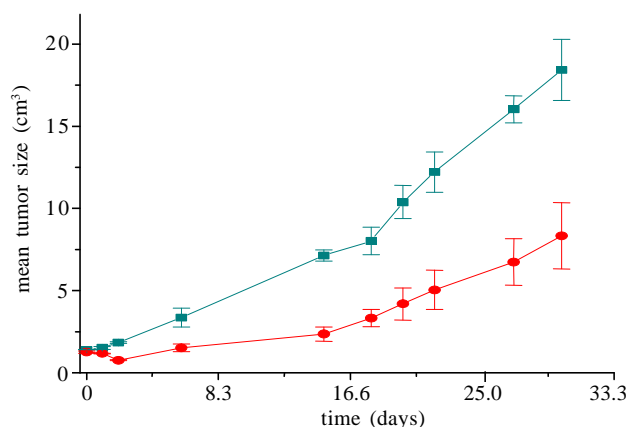


**Figure 2.** Tumor growth curves corresponding to both MAB IOR EGF/r3-treated group (solid circle) with a single intravenous dose (8 mg/kg), and PBS-treated control group (solid square), in tumor bearing nude mice. Kinetics pattern shows a tumor growth delay after IOR EGF/r3 treatment.

that these slopes belong to different family of growth curves ( $p = 0.003$ ). A satisfactory delay of tumor growth rate was shown with a 13% TGD ratio, which denoted a potential of this monoclonal for tumor growth inhibition (see Figure 2), even though significant remission of the tumor mass was not evident over time other than the first 48 hours, as can be derived from negative slope of best fitted polynomial function within 0-48 hours (see Table 4).

Figure 3 depicts photomicrographs of immunohistochemical staining for both Ki67 antigen and PCNA molecule in malignant cells at 48 hours after dosing when higher AI/MI ratio was observed. As can be seen, these two proliferation markers (i.e, Ki67 and PCNA) were better detected in the PBS control rather than in the IOR EGF/r3-treated slices, suggesting a higher AI/MI ratio in the latter and supporting our thesis of IOR EGF/r3-driven induction of any PCD in treated tumors after stopping cell-cycle progression. Table 5 shows the estimated average Ki67 and PCNA values as percentage at each time point according to immunostaining of specimens. Notice the irregular behavior over time from the observed PCNA

**Table 3.** Comparison of tumor growth curves from both groups. Statistical analysis was achieved by correlation and multiple regression analysis of both profiles using a polynomial function as a model.

<b>PBS-treated control group (<math>r^2 = 0.834</math>)</b>				
<b>Slope = <math>9.394 \cdot 10^3 (\pm 1.15 \cdot 10^3)</math></b>				
Variance Source	DF	QSS	F	p
Between groups	9	190.53	31.51	0.001
Regression	1	170.1	66.275	0.001
Deviation of regression	8	20.52	3.819	0.010
Within groups	20	13.43	----	----
<b>Total</b>	<b>29</b>	<b>208.97</b>	----	----

<b>MAB IOR EGF/r3-treated group (<math>r^2 = 0.949</math>)</b>				
<b>Slope = <math>1.345 \cdot 10^2 (\pm 6.56 \cdot 10^4)</math></b>				
Variance Source	DF	QSS	F	p
Between group	9	355.33	65.77	0.001
Regression	1	348.68	419.65	0.001
Deviation of regression	8	6.647	1.384	NS
Within groups	20	12.006	----	----
<b>Total</b>	<b>29</b>	<b>367.34</b>	----	----

DF means degree of freedom; QSS means sum of quadratic standard error; F is Fischer's number; p is probability level; NS means non significant difference.

**Table 4.** Analysis of slopes from both tumor growth curves, by ANOVA of regression, using two sections of both curves, from 0 to 48 hours and from 144 to 720 hours.

Parameters	PBS	MAB IOR EGF/r3	p
<b>[0 to 48 hours]</b>			
Slope	$4.305 \cdot 10^{-3}$	$-1.04 \cdot 10^{-2}$	0.0001
Intercept	1.284	1.308	
<b>[144 to 720 hours]</b>			
Slope	$1.426 \cdot 10^{-2}$	$1.248 \cdot 10^{-2}$	NS
Intercept	0.5047	-1.314	

\*Statistically significant difference between groups was observed during first 48 hours.

marker, which becomes increasingly difficult to make any prediction on tumor response. In fact, these PCNA values lagged behind current phase of cell cycle, overestimating actual cell proliferation in comparison with Ki67 antigen detection. Conversely, the Ki67 marker permitted us to postulate a pattern in relation to the previously observed MI and also tumor growth time courses.

A moderate degree of inverse correlation between Ki67 antigen and AI to MI ratio was observed in the MAB-treated group, which yielded new evidence concerning the idea of postulating IOR EGF/r3 as an inducer of cell-

**Table 5.** Statistical comparison between treated and untreated control group, for both PCNA and Ki67 antigen. A paired t-student test, with 5% probability, was used. PCNA and Ki67 values were calculated with regard to 1000 cells.

Time (h)	PCNA mean values (± SD)		p level	Ki67 mean values (± SD)		p level
	PBS	IOR EGF/r3		PBS	IOR EGF/r3	
0	5.7 (±1.2)	6.2 (±0.8)	NS	2.9 (±0.7)	3.4 (±0.5)	NS
48	6.2 (±1.1)	11.1 (±1.6)	0.012	2.2 (±0.8)	1.3 (±0.6)	NS
144	9.4 (±0.8)	3.7 (±0.4)	0.002	3.8 (±1.2)	1.2 (±0.4)	0.024
360	7.5 (±1.4)	4.3 (±0.7)	0.038	4.2 (±0.7)	2.1 (±0.7)	0.021
480	9.5 (±0.6)	3.1 (±0.3)	0.001	4.7 (±0.5)	2.1 (±0.6)	0.004
720	10.2 (±1.4)	5.6 (±1.5)	0.018	6.1 (±1.2)	1.8 (±1.0)	0.009

NS means no-significant differences between groups.

cycle arrest and pro-apoptotic response, even though MI values were determined following morphometric analysis whereas immunostaining for Ki67 antigen often picks out a maximum label at G<sub>2</sub>/M boundary of the cell cycle. Notably, Ki67 values in the MAb-treated group declined

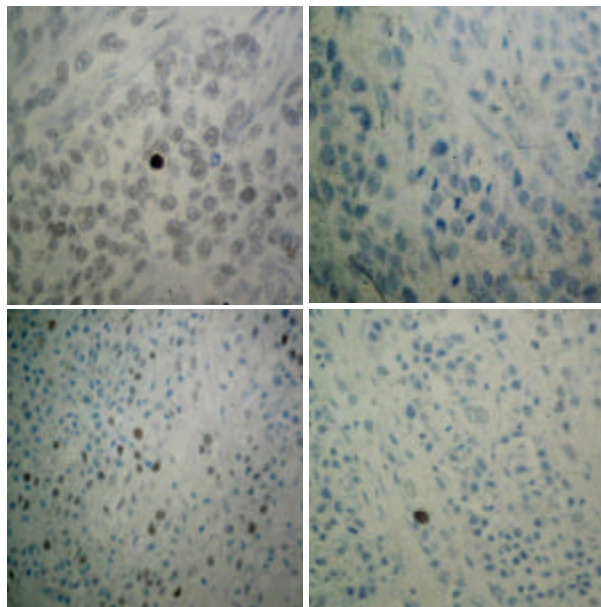


**Figure 3.** Immunohistochemical staining for both Ki67 antigen using NCL-Ki67-MM1 (upper panels) and PCNA using NCL-PCNA (lower panels), in tumor specimen from either PBS-treated control (left hand) or IOR EGF/r3-treated (right hand) xenograft, 48 hours after dosing. Paraffin sections. Note intense nuclear staining of proliferating H125 cells, particularly in controls.

below baseline up to about 144 hours after treatment and then recovered from day 15 onward. As expected, such proliferation markers confirmed the assumptions derived from former AI/MI assessments.

## Discussion

Little is known of the role of PCD in the response of tumors to different therapeutic modalities in spite of the fact that almost 30 years ago cells with the features of apoptosis were demonstrated in the tumors of treated animals (12). Much of what has been done in recent years has primarily involved cells treated in vitro. Although, much has been learned about basic mechanisms from such studies, a critical question that remains

unanswered is whether these mechanisms extrapolate to tumors treated in vivo. This study was conducted to assess the magnitude and time course of the apoptosis induction in carcinomas treated with a promising agent (viz, monoclonal antibody IOR EGF/r3), in order to determine whether this mode of cell death can be involved in its therapeutic action.

Earlier summaries of in vivo studies on HiFi colon adenocarcinomas, at the Sloan Kettering Cancer Center of New York, report that these tumor cells display the features of apoptosis following exposure to the anti-EGFr human-to-murine chimeric MAb C225 (13). Furthermore, in vitro studies on cultured H125 cells showed the presence of apoptotic bodies following IOR EGF/r3 treatment and, more recently, in vivo studies using both murine IOR EGF/r3 and its humanized version showed similar pro-apoptotic pattern on A431 cells (8). Nonetheless, it has also been shown that the appearance of apoptosis in treated cells is a very dynamic and complex process, making it difficult to readily assess the total proportion of apoptotic cells.

The kinetics of apoptosis induction by IOR EGF/r3 in the H125 cells, confirms that several factors may contribute to the proportion of apoptotic cells visualized at any time point. This kinetic pattern is in contrast to that seen after ionizing radiation and other therapy options (10, 14). One explanation may be the pharmacokinetics of the drug uptake by the tumor cells, which probably occurs asynchronously and over a longer time compared to radiation, where the entire dose is delivered within a few minutes.

Alternatively, the kinetics of apoptosis following MAb treatment may be due to cell cycle specificity for induction of this mode of cell death as suggested by Barry et al. (15). It is possible that there are other modes of cell death and that a high proportion of cells in these tumors died by what is referred to as reproductive cell death, where cells simply stop dividing after completing one or more abnormal post treatment divisions. It is not clear that this mode of

cell death occurs in these tumors since it cannot be visualized. However, it is consistent with the fact that the MI fell below the levels before IOR EGF/r3 injection and displayed a plateau during the next 20 days, and then suddenly showed a rapid recovery.

A possible explanation for this terminal proliferation behavior is related to the heterogeneous angio-architecture of these tumors and therefore the heterogeneous distribution of macromolecules into these tumors, as previously was suggested (16-18), along with the better condition found by resistant clones for their malignancy due to death of the treated sensitive ones. It reinforces the requirements of multiple dosage regimens in order to obtain sustained steady-state drug levels over longer time periods, that permit us a complete saturation of the over-expressed EGFr on target tumor cells. In this context, we firmly believe that using chemotherapy along with IOR EGF/r3 immunotherapy should yield a better global clinical outcome.

The AI observed at any specific time most likely underestimates the total proportion of cells that undergo apoptosis throughout the time course of the experiment. This might be due to the fact that two competing processes are going on: as apoptotic cells are continuously formed they are quickly phagocytosed, perhaps accounting for the ultimate decline in AI observed after the peak near to 20 days. Thus, the true proportion of cells deleted through apoptosis may be much higher, considering that the life time for visualization of an apoptotic cell may be as short as 3 hours (19). Moreover, some tumor cells may be resistant to apoptosis; it is now well established from a number of studies that the propensity for apoptosis in response to a variety of agents used in cancer therapy, including MABs against EGFr, is highly dependent on the oncogenic status of the cell.

The effects of IOR EGF/r3 on tumor growth were measured to test the role of apoptosis on tumor response. All treated tumors displayed a fairly evident growth delay after a single dose of 8 mg/kg. However, the exact relationship between apoptosis induction and this tumor response measured in terms of growth delay is not clear; nevertheless, this dose counteracted the tumor mass progression compared to the control group, but they continued to grow after a slight delay even though substantial apoptosis was induced with this dose. There are two possible explanations for this apparent discrepancy. First, as discussed above, the evaluation of apoptosis from the histological sections may underestimate the total proportion of cells that underwent apoptosis during the time course studied. Second, since the re-growth kinetics also depend strongly on the rates of proliferation of surviving clones, apoptosis in the tumors

that received a single dose could be offset by new cell division of these surviving clones after clearance of the monoclonal antibody. The MI scored on the same sections as used for the analysis of apoptosis confirmed that cell proliferation was suppressed to a not very high extent and rebounded near 30 days. Thus, resumption of spontaneous apoptosis in these tumors apparently relied on resumption of cell proliferation.

The assessment of cell proliferation by detection of Ki67 antigen has been shown to be of some prognostic value. NCL-Ki67-MM1 label Ki67 antigen in the granular components of the nucleolus during late G1, S, G2 and M phases of cell cycle, and several reports have suggested that there is a strong correlation between Ki67 index and grade histopathology of tumors. Interestingly, the prognosis of this cell-cycle associated marker has been found comparable to [ $H^3$ ] thymidine assay as a sound cell proliferation criterion.

On the other hand, PCNA is a 36 kDa protein which is highly conserved between species and functions as a cofactor for DNA polymerase delta in both S phase and also in DNA synthesis associated with DNA damage repair mechanism. Yet, PCNA may also be detected in non-cycling cells at G0 phase inasmuch as this molecule has a half-life in excess of 20 hours. Therefore, these values on Table 5 should be seen with caution for further interpretation.

It now appears that PCNA is also a communication point between a variety of important cellular processes including cell cycle control, DNA replication, and at least one apoptotic pathway. The dynamic movement of PCNA on and off the DNA renders this protein an ideal communicator for a variety of proteins that are essential for DNA metabolic events in eukaryotic cells (20). Even though the primary function of PCNA may be to act as a processivity factor for polymerases, a cell decision as to what type of DNA synthesis has to be carried out for its survival might be addressed by the various interactions of PCNA with other proteins. This eventually leads to decisions such as the direction of PCNA towards faithful replication (preceding cell division), various types of repair processes, or even a stop in DNA synthesis events (cell cycle arrest) that could determine a final cell decision to go into PCD pathway, thus allowing a fine tuning of the interplay of these cardinal processes. We have to learn more about the details of the interactions between PCNA and the various components of cell cycle and how they are regulated.

In summary, we have confirmed the observations of others with regard to the apoptosis inducing properties of the MAB IOR EGF/r3 and extended these observations to the in vivo situation using the tumor bearing nude mice as a relevant animal model at disease-state. The magnitude

of this effect implies that this mode of cell death could play a role in tumor response, especially in tumor delay following treatment with IOR EGF/r3. Thus, understanding the pathways responsible for regulating the propensity for tumor cells to undergo apoptosis as well as its kinetics behaviors could ultimately enable the design of strategies for modulating PCD according to the optimization of IOR EGF/r3's dosage regimens with therapeutic advantage.

## Resumen

La apoptosis tiene un importante papel en la inmunoterapia del cáncer. En este estudio, hemos caracterizado la cinética de inducción de apoptosis en xeno-injertos de carcinoma de pulmón humano, línea tumoral H-125, luego de administrar el anticuerpo monoclonal anti-factor de crecimiento epidérmico IOR EGF/r3. Ratones atómicos que portan un tumor recibieron intravenosamente una dosis única de 8mg/kg de IOR EGF/r3, posteriormente se tomaron muestras del tumor hasta los 30 días siguientes al tratamiento. La apoptosis fue medida mediante análisis morfológico de las secciones histológicas correspondientes a cada muestra de tumor para el intervalo de muestreo establecido. Los resultados muestran una significativa apoptosis en los tumores en los 6 días siguientes a la administración del monoclonal, alcanzando un máximo a los 20 días postratamiento. La respuesta cinética resultó bien extendida, con visualización de células en apoptosis durante todo el período de muestreo. El transcurso temporal del índice de apoptosis muestra una diferencia significativa respecto al índice mitótico. Finalmente, la apoptosis inducida por este monoclonal fue relacionada con el retardo del crecimiento tumoral, indicándose un probable arresto del ciclo celular y una consecuente inhibición de la progresión tumoral, lo cual fue corroborado por los bio-marcadores PCNA y Ki67.

## Acknowledgments

This work was supported by the Center of Molecular Immunology, the Department of Pathology, Royal Victoria Infirmary, University of Newcastle upon Tyne, and in part by grant A023 from Alma Mater project. The skillful technical assistance of Mrs. Amelia Capote, Mr. Armando López, and Mr. Dariel Morales is gratefully acknowledged.

## References

1. Kerr JFR, Winterford CM, Harmon BV. Apoptosis: Its significance in cancer and cancer therapy. *Cancer*, 1994;73: 2013-26.

2. Lane DP. A death in the life of p53. *Nature (Lond.)*, 1993;362: 786-7.
3. Hsu B, Marin MC, Brisbay S, McConnell K, McDonnell TJ. Expression of bcl-2 gene confers multi-drug resistance to chemotherapy-induced cell death. *Cancer Bull.* 1994;46: 125-9.
5. Stephens LC, Ang KK, Schultheiss TE, Milas L, Meyn RE. Apoptosis in irradiated murine tumors. *Rad. Res.* 1991;127: 308-16.
6. Kyprianou N, English HF, Isaacs JT. Programmed cell death during regression of PC-82 human prostate cancer following androgen ablation. *Cancer Research.* 1990;50:3748-53.
7. Arends MJ, McGregor AH, Wyllie AH. Apoptosis is inversely related to necrosis and determines net growth in tumors bearing constitutively expressed myc, ras, and HPV oncogenes. *Am. J. Pathology.* 1994;144:1045-57.
8. Crombet T, Rak J, Perez R, Vilorio-Petit A. Antiproliferative, antiangiogenic and proapoptotic activity of hR3: A humanized anti-EGFr antibody. *Int. J. Cancer.* 2002;101(6):567-575.
9. Fernández A, Pérez R, Macías A, Velanda A, Álvarez I, Ramos M, Velozo A. Generación y caracterización primaria de anticuerpos monoclonales contra el receptor del factor de crecimiento epidérmico. *Interferón y Biotecnología.* 1989; 6(3):289-298.
10. Meyn RE, Stephens LC, Hunter NR, Milas L. Kinetics of cisplatin-induced apoptosis in murine mammary and ovarian adenocarcinomas. *Int. J. Cancer.* 1995;60:725-29.
11. Grizzle JE, Allen DM. Analysis of growth and dose response curves. *Biometrics* 1969;25:357- 81.
12. Searle J, Lawson TA, Abbott PJ. An electron- microscope study of the mode of cell death induced by cancer chemotherapeutic agents in populations of proliferating normal and neoplastic cells. *J. Pathology* 1975;116:129-38.
13. Wu XP, Rubin M, Fan Z, Deblasio T, Soos T, Koff A, Mendelsohn J. Involvement of P27(KIP1) in G(1) arrest mediated by an anti- epidermal growth factor receptor monoclonal antibody. *Oncogene* 1996;12(7):1397-1403.
14. Stephens LC, Hunter NR, Ang KK, Milas L, Meyn RE. Development of apoptosis in irradiated murine tumors as a function of time and dose. *Rad. Res.* 1993;135:75-80.
15. Barry MA, Behnke CA, Eastman A. Activation of programmed cell death by cisplatin, other anticancer drugs, toxins and hyperthermia. *Biochemistry and Pharmacology* 1990;40:2353-62.
16. Ahlstrom H. Anatomy and permeability of tumor vessels. An experimental study in nude rats with the aim of increasing the uptake of MAb anti- CEA in human colonic cancer. PhD Thesis, Department of Diagnostic. Uppsala University, 1988;S-75185, ISBN 91-7900-448-2, Sweden.
17. Jain RK, Baxter LT. Mechanism of heterogeneous distribution of MAb and other macromolecules in tumors: Significance of elevated interstitial pressure. *Cancer Research* 1988;48:7022-32.
18. Jain RK. Physiological barriers to delivery of MAb and other macromolecules in tumors. *Cancer Research* 1990;50:814-19.
19. Bursch W, Paffe S, Putz B, Barthel G, Schulte-Hermann R. Determination of the length of the histological stages of apoptosis in normal liver and in altered hepatic foci of rats. *Carcinogenesis* 1990;11:847-53.
20. Jónsson ZO, Hübscher U. Proliferating cell nuclear antigen: more than a clamp for DNA polymerases. *Bioessays* 1997; 19(11):967-975.